Renal Tubular Receptor Imaging with Iodine-131-Labeled Peanut Lectin: Pharmacokinetics and Renal Clearance Mechanism in Animals

Graeme R. Boniface, Mavanur R. Suresh, David J. Willans, Yun K. Tam, Alec Shysh, B. Michael Longenecker, and Antoine A. Noujaim

Faculty of Pharmacy and Pharmaceutical Sciences, Department of Immunology, University of Alberta; and Department of Laboratory Medicine, Edmonton General Hospital, Edmonton, Alberta, Canada

Intravenously administered peanut lectin (PNA), iodinated with ^{131}I ([^{131}I]PNA), is rapidly cleared from the plasma by the kidneys in dogs (clearance [total body] = 17.52 ± 8.74 ml/min). Dynamic gamma camera renal scintigraphy demonstrated renal accumulation and excretion phases of the [^{131}I]PNA renogram in dogs and rabbits (% injection dose-at-peak = 21.8 ± 3.3% and 19.6 ± 4.3%, time-to-peak = 44.6 ± 4.8 min and 37.2 ± 6.9 min, respectively). Immunoperoxidase staining of kidney sections, following i.v. administered PNA, demonstrated predominant accumulation by the proximal tubules of mice, rabbits, and dogs. The basement membrane was intensely stained at early times p.i. while intracellular and luminal PNA was evident within 1 hr. Urine analysis confirmed the presence of intact [^{131}I]PNA in the bladder contents, while protein degradation products, and a small percentage of the free iodide (<5%) were noted within 1 hr p.i. The relative proportion of free iodide increased at later times p.i. (>6 hr). A receptor mediated excretion mechanism is proposed for the clearance of PNA and may be useful for the study of renal tubular function.

J Nucl Med 27:668–676, 1986

Recently, much evidence has been produced to implicate the Thomsen-Friedenreich (T-F) antigen as an important tumor-associated antigen in many animal and human carcinomas (*1–4*). The immunodeterminant group of this antigen is the β-D-galactosyl-(1 → 3)-α-*N*-acetyl-D-galactosamine (β-D-Gal-(1 → 3)-α-GalNAc) moiety (*5*). This antigen is found in an asialo or "unmasked" form in a wide variety of embryologic and malignant cell types (*6,7*).

Peanut agglutinin (PNA) is a plant protein of 105,000–110,000 mol wt which exhibits specific binding to the T-F antigen as well as the terminal disaccharide of the asialo-GM_1 antigen (β-D-Gal-(1 → 3)-β-GalNAc) (*8*). Histologic studies using PNA have demonstrated binding sites on the luminal surface of renal tubules (*9–13*) and these techniques have been useful in delineating morphologic heterogeneity in kidney tissue sections. PNA has also been used for the identification of receptors on various normal and malignant cell types in animal and human tissues (*2–4,7*)

Radioiodinated PNA has been used recently in our unit as a radioimmune probe for the in vivo detection of solid tumors and metastases in mice and a selected number of human patients with metastatic disease (*14–18*). In preliminary biodistribution experiments in mice, rapid plasma clearance and renal accumulation were noted after the i.v. injection of iodine-125 (^{125}I) PNA (*19*) and was also documented in humans after iodine-131 (^{131}I) PNA administration (*15,16*). This study was undertaken to investigate the plasma pharmacokinetics and the mechanism of renal clearance of i.v. administered [^{131}I]PNA in animal models.

MATERIALS AND METHODS

Labeling of PNA with ^{131}I

Iodination of PNA was achieved by the iodogen method. PNA* (1 mg) was incubated in a tube contain-

Received May 28, 1985; revision accepted Jan. 21, 1986.

For reprints contact: Antoine A. Noujaim, MD, Faculty of Pharmacy and Pharmaceutical Sciences, Dept. of Immunology, University of Alberta, Edmonton, Alberta, Canada.

ing 10 μg of iodogen† coated on the surface. Na ^{131}I‡ (185–550 MBq) in 0.5*M* phosphate buffer was added and the tube was incubated at room temperature for 60 min. The solution was removed and placed in 50 μl 1*M* KI and subsequently passed through a gel column (1.5 × 25 cm. Biogel P6-DG§) using 0.05*M* phosphate buffered saline (PBS) as eluant. The void volume was collected and the activity was determined in an isotope dose calibrator, calibrated for ^{131}I. Labeling efficiency was determined and aliquots were assayed for both immunoreactivity (asialo-GM_1-synsorb binding assay) and protein association (trichloroacetic acid [TCA] precipitation).

Trichloroacetic Acid Precipitation

One hundred microliters of each sample were added to 1 ml of cold (4°C) 10% bovine serum albumin (BSA). One milliliter of cold 25% TCA was added to this and samples were allowed to stand in an ice bath at 4°C for 15 min. The samples were then centrifuged at 1,000 *g* for 10 min, the supernatant aspirated, and the pellet and supernatant were both counted in a gamma counter with the % activity in the pellet calculated.

Asialo-GM1 Synsorb Binding Assay

One hundred microliters of each sample were diluted to 1.0 ml with 5 m*M* PBS. This was added to 50 mg of asialo-GM_1-synsorb* in an Eppendorf mini-tube and 50 μl were immediately withdrawn for counting in a gamma counter. The tubes were placed on an inversion mixer and gently mixed for 12 hr after which 50 μl of supernatant were withdrawn and counted. The % asialo-GM_1-synsorb binding was calculated by comparing the counts in the supernatant at 0 and 12 hr.

Stability Studies

The stability of [^{131}I]PNA, stored at room temperature, and when incubated in plasma or urine at 4 or 37°C, was determined by TCA precipitation for 5 days following radioiodination of four separate batches of [^{131}I]PNA. These results were used to determine a suitable shelf-life for [^{131}I]PNA and to determine suitable storage conditions for the assay of [^{131}I]PNA in biologic samples.

ANIMAL STUDIES

Pharmacokinetics

Two hundred micrograms of freshly prepared [^{131}I]PNA (25–35 MBq) were injected i.v. into four anesthetized male dogs (17–21 kg) and blood samples (2 ml) were drawn into heparinized tubes from a contralateral leg vein at 3, 5, 7, 10, 12, 15, 20, 30, 45 min and 1, 1.5, 2, 3, 4, 6, 9, 12, 24, 48 hr p.i. Plasma was generated by centrifuging the whole blood at 1,000 *g* for 10 min. Standard plasma aliquots (0.5 ml) were counted in a gamma counter along with standards of the injected material. Aliquots of plasma were treated with TCA, as previously described, and the % protein-bound radioactivity was calculated by comparing the counts in the protein pellet to those in the supernatant (free I^-). Plasma activity/time curves were generated for both total radioactivity and protein-bound radioactivity, and these were analyzed by a computer NONLIN bi-exponential curve fitting program. Standard pharmacokinetic parameters were derived assuming a two-compartment model described by the pharmacokinetic equation (*19*):

$$A = A_0e^{-\alpha t} + B_0e^{-\beta t}.$$

The half-life ($t_{1/2}$) of both the fast (α) and slow (β) exponentials were calculated from the stripped curve:

$$t_{1/2}\,\alpha = \frac{0.693}{\alpha}$$

and

$$t_{1/2}\,\beta = \frac{0.693}{\beta}.$$

The volume of distribution (Vd) was calculated from the plasma activity/time curves from the intercept of the curve ($A_0 + B_0$) at $t = 0$, and relating this to the total injected dose:

$$Vd = \frac{\text{Total dose injected}}{A_0 + B_0}.$$

The area under the plasma curve (AUC) was calculated using the equation:

$$AUC = \frac{A_0}{\alpha} + \frac{B_0}{\beta}$$

and the clearance (total body) [CL/Tb] calculated from the equation:

$$CL/Tb = \frac{\text{Total dose injected}}{AUC}.$$

Red cell binding was determined on all blood samples by counting aliquots of the packed cell volume (0.5 ml) that had been washed and respun ×3 in PBS. Counts were compared with the plasma aliquots and % red-cell binding determined.

Urine was collected throughout the study by bladder catheterization (0–9 hr) and by metabolic cage isolation (9–48 hr). Total radioactivity was determined for each collection period 0–1, 1–3, 3–6, 6–9, 9–24, and 24–48 hr p.i., along with % protein-bound radioactivity (TCA precipitation) and asialo-GM_1 synsorb binding. Representative 1-hr urine samples were analyzed by gel column chromatography (Biogel P 150§, 2.5 × 50 cm) with PBS as eluent, using a dual channel monitor to measure levels of protein and radioactivity (280 nm uv absorbance, SCA calibrated for ^{131}I).

Renal Kinetics

During the study each dog was placed supine under a gamma camera¶ interfaced to a computer (ADAC

CAM II). Dynamic frames (64 × 64 matrix) was accumulated at 30-sec intervals for 60 min p.i. Regions of interest (ROIs) were generated over each kidney, the heart pool, and adjacent kidney background areas. Background-corrected renal activity/time curves were analyzed by an exponential curve fitting program ($A = A_0[1 - e^{-\lambda r}]$) and the renal uptake parameters (% injected dose-at-peak, time-to-peak, and $t_{1/2}$ uptake) were determined.

Static images (150,000 counts, 128 × 128 matrix) were acquired over the kidneys and bladder at 1, 2, 3, and 24 hr p.i. immediately before and after bladder catheterization. The relative activity in each kidney and the bladder were determined from background corrected ROIs. These were corrected for absolute counts (% inj. dose) by counting aliquots of the aspirated urine, along with injection standards, and relating the counts in the pre- minus postvoid bladder ROI (i.e., collected urine counts) to those in each kidney ROI.

Comparative Studies

Dynamic gamma camera/computer studies were acquired as above after i.v. injection of 100 μg/18 MBq [^{131}I]PNA into anesthesized rabbits (NZW). Activity/time curves were generated over the kidneys, bladder, and heart pool, and renal uptake parameters were determined as previously described. Static scintiphotos were acquired at 30 and 60 min p.i. to demonstrate in vivo biodistribution. The biodistribution and renal kinetics were determined for animals pretreated with probenecid (20 mg i.p.), furosemide (2 mg i.p.), rabbit anti-PNA IgG antibodies** (120 μg i.v.), and epiglycanin (160 μg i.v.) 60 min prior to i.v. injection of [^{131}I]PNA. Kinetic parameters and kidney/liver ratios were compared with those from untreated controls.

Immunoperoxidase Tissue Histology

Doses of 1–100 μg PNA were injected i.v. into CAF1/J mice, dogs, and rabbits. Animals were killed at various time intervals p.i. (30 min –24 hr), the kidneys were removed and washed in cold saline (0°C). The kidneys were imbedded in OCT†† and frozen in isopentane at −70°C. Cryostat sections were fixed in acetone and washed with PBS. The sections were incubated in diluted rabbit serum for 20 min to minimize nonspecific staining. Natural avidin substances were blocked by application of Avidin reagent‡‡ for 15 min, washed and treated with Biotin blocking reagent‡‡ for a further 15 min. Sections were then incubated for 30 min wth a 1/50 dilution of goat anti-PNA‡‡. A 30- min incubation with biotinylated antigoat IgG, followed by a 60-min incubation with Avidin peroxidase reagent†† were subsequently performed. The sections were finally incubated for 5 min in freshly prepared DAB-H_2O_2 solution. Duplicate immunoperoxidase stained slides were either counterstained with Harris's Hematoxylin or not counterstained.

RESULTS

PNA was readily radioiodinated with ^{131}I and labeling efficiencies of 45–65% were routinely achieved. TCA precipitation assays of the void volume fraction consistently revealed >98% of the radioactivity was protein bound and asialo-GM_1 synsorb binding assays indicated >96% immunoreactivity, that was competitively inhibitable by D-galactose. A loss of ~1%/day of radioiodide was demonstrated when [^{131}I]PNA was stored at 20°C. Iodine-131 PNA stored in plasma or urine at 4°C revealed an insignificant loss (<1%) in protein-bound radioactivity up to 5 days following iodination, however, when incubated at 37°C, a decrease of 1.5–2% in TCA precipitable radioactivity/day was observed in both plasma and urine.

Normalized plasma activity/time curves of both total radioactivity and protein-bound radioactivity (TCA precipitation data) in dogs (Fig. 1) revealed significantly different rates of clearance ($p < 0.05$) due to the increasing contribution of free ^{131}I with time. At 2 hr p.i., 67 ± 4% of the remaining radioactivity in the plasma was protein-bound, while at 24 hr, this had diminished to 10 ± 2%. NONLIN biexponential curve fitting of both curves revealed that the curves were best described by a two-compartment model and the exponential parameters were calculated (Table 1). Protein-bound radioactivity rapidly diminished from the plasma compartment (CL/Tb = 17.52 ± 8.74 ml/min) while total radioactivity showed significantly slower clearance (CL/Tb = 8.25 ± 3.72 ml/min). The apparent volume of distribution (Vd) was low (Vd = 1.27 ± 0.48 l) indicating that [^{131}I]PNA distribution is largely confined to the plasma following i.v. injection. No significant red cell binding was been in any of the blood samples (<1%) throughout the study period.

Whole-body scintigraphy revealed that plasma clearance was primarily due to renal accumulation and excretion, with no significant uptake demonstrated by the liver or other organs at early time periods. At later time points (>6 hr p.i.), radioactivity was noted in the thyroid, salivary glands, and stomach, an observation consistent with the presence of free ^{131}I. KI blockade was not used in these experiments. Activity/time curves generated over the kidneys of dogs indicated rapid renal accumulation of [^{131}I]PNA (time-to-peak = 44.6 ± 3.7 min, % inj. dose-at-peak 21.8 ± 3.3%) (Table 2). Exponential curve fitting of the uptake slope revealed consistent values of slope-to-peak and $t_{1/2}$ uptake estimates, for control dogs and rabbits (14.2 ± 2.8 min and 13.7 ± 3.6 min, respectively).

Gel chromatographic profiles of urine aspirated at 1 hr p.i. revealed significant protein-associated counts, which co-eluted with the parent PNA fraction along with smaller molecular weight fragments and a small free ^{131}I peak (Fig. 2). TCA precipitation confirmed the

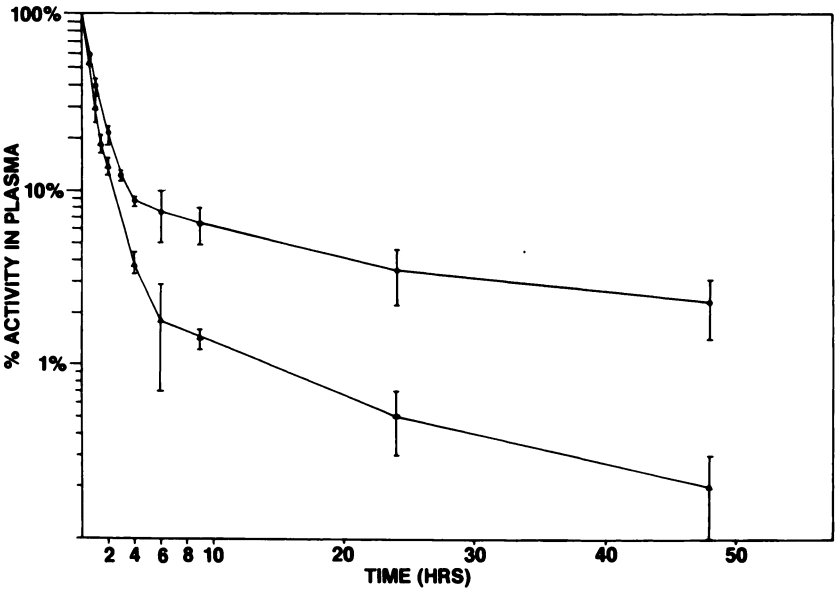

FIGURE 1
Normalized plasma activity/time curves following i.v. injection of [^{131}I] PNA in dogs (mean ± s.d., N = 4). Bi-exponential curve fitting estimates of total radioactivity (●—●) and protein-bound radioactivity (TCA ppt assay (▲—▲)

quantity of the protein-bound counts and this protein appeared functional in respect to asialo-GM_1 synsorb binding (Table 3). Cumulative urine analysis resulted in recovery of 73.5 ± 9.8% of the injected dose of radioactivity within 48 hr p.i. During the early periods (<6 hr), >75.4% of the urine radioactivity was protein bound of which >51.8% appeared to be intact [^{131}I] PNA as determined by asialo-GM_1 synsorb binding assay. At later time points increasing levels of free ^{131}I were noted. The lower molecular weight protein fragments, observed by gel column chromatography, were not further characterized.

The total radioactivity remaining in the kidneys at 1, 2, 3, 6, and 24 hr p.i., as determined from static images, demonstrated diminishing radioactivity, that paralleled that within plasma. This indicated that the renal activity was excretory in nature, and residual renal fixation of [^{131}I]PNA was not evident during the study period (Fig. 3). Histologic preparations confirmed decreasing renal PNA concentration with time. Iodine-131 PNA kidney uptake and clearance was significantly reduced when D-galactose (2.5 g loading dose, 50 mg/min infusion) was administered concurrently. The % inj. dose-at-peak in both kidneys was diminished (10.9%) when compared with controls (21.8%), while the % inj. dose in bladder at 60 min p.i. was also reduced (4.7% as compared with 12.8% in controls) (Fig. 4).

In rabbits, renal studies were undertaken with controls and animals pretreated with probenecid, furosemide, anti-PNA IgG antibodies, and epiglycanin (a PNA binding glycoprotein) (Table 2). No significant difference in renal uptake parameters, % inj. dose in bladder (60 min p.i.), or kidney/liver ratio were seen when probenecid (20 mg i.p.) was injected 1 hr prior to [^{131}I] PNA administration. Furosemide (2 mg i.p.) resulted in a minor increase in % inj. dose in bladder at 60 min p.i., however, no change in the remaining parameters was demonstrated. This is most likely due to an increase in kidney/bladder transit rate as a result of diuresis. The prior injection of rabbit anti-PNA (120 μg i.v.) and epiglycanin (160 μg i.v.), however, had dramatic effects on the biodistribution of [^{131}I]PNA. Predominant liver accumulation was demonstrated after pretreatment with both agents, that resulted in significant reduction in the renal activity (Fig. 5). Quantitative values for the renal parameters were thus difficult to assess with any degree of accuracy due to <5% of the injected dose being contained in the kidneys.

TABLE 1
Normalized Biexponential Curve Fitting Estimates of Plasma Radioactivity (Mean ± s.d., N = 4)*

Item	A_0 (%)	$T_{1/2}\,\alpha$ (hr)	B_0 (%)	$T_{1/2}\,\beta$ (hr)	Vd (l)	Cl/TB (ml·min^{-1})
Total plasma radioactivity R = 0.998†	86.32 ± 8.27	0.45 ± 0.09	20.10 ± 8.21	14.78 ± 2.81	1.27 ± 0.48	8.25 ± 3.72
Protein-bound radioactivity R = 0.996†	68.23 ± 7.41	0.31 ± 0.03	39.75 ± 7.81	1.19 ± 0.16	1.27 ± 0.48	17.52 ± 8.74

* Using expression $A = A_0e^{-\alpha t} + B_0e^{-\beta t}$.
† Correlation coefficient.

TABLE 2
[^{131}I]PNA Renal and Bladder Kinetics in Dogs and Rabbits*

Item	Dogs		Rabbits				
	Controls (N = 4)	D-Galactose (N = 2)	Controls (N = 4)	Probenecid (N = 2)	Furosemide (N = 2)	Anti-PNA (N = 2)	Epiglycanin (N = 2)
Time-to-peak (min)	44.6 ± 4.8	43.7 ± 3.8	37.2 ± 6.9	35.2 ± 2.8	34.8 ± 4.7	>60	>60
% Inj. dose-at-peak (Both kidneys)	21.8 ± 3.3	10.9 ± 2.1	19.6 ± 4.3	18.3 ± 4.1	20.1 ± 2.6	1.2 ± 0.6	5.9 ± 3.8
$T_{1/2}$ uptake (min)	14.2 ± 2.8	15.2 ± 1.9	13.7 ± 3.6	14.6	13.9	—	—
% Inj. dose in bladder (1 hr p.i.)	12.8 ± 5.3	4.7 ± 2.1	12.6 ± 3.9	13.8 ± 3.2	17.2 ± 2.8	<1.0	1.8
Kidney/liver ratio (1 hr p.i.)	17.5 ± 2.8	14.2 ± 2.6	18.9 ± 1.8	17.3 ± 2.4	16.2 ± 3.1	<0.01	0.03

* Controls compared with animals pretreated with D-galactose (2.5 g loadize dose, 50 mg/min infusion), probenecid (20 mg i.p.), furosemide (2 mg i.p.), anti-PNA (120 μg i.v.), and epiglycanin (160 μg i.v.).

Immunoperoxidase studies of mouse kidneys showed a changing pattern of staining. At 10 min p.i., PNA was demonstrated in almost all outer cortical proximal tubules, and also within collecting ducts (Fig. 6 A,B). No interluminal PNA could be visualized, and glomeruli were virtually negative. The tips of renal papillae were poorly visualized but cytoplasmic marking of tubular epithelial cells in the distal portions of the pyramids was seen at all time intervals. Marking of the proximal convoluted tubules consisted of linear prominence along the outer border as well as difuse epithelial staining. Marking was maximal at 2–6 hr, but only trace residual PNA was seen at 24 hr. Medullary activity diminished in a similar manner.

DISCUSSION

PNA was readily iodinated with ^{131}I, and the radioiodinated protein appears to be stable up to 5 days following iodination when stored in urine or plasma at 4°C. This confirms previously reported stability studies on [^{131}I]PNA stock solution (*21*), and allows the accurate analysis of biologic samples containing [^{131}I]PNA up to several days following collection.

After i.v. injection, [^{131}I]PNA is rapidly cleared from the plasma by the kidneys and excreted into the bladder. Microscopic studies with the immunoperoxidase technique have revealed that the proximal tubular cells are largely responsible for the extraction of PNA from the plasma and significant amounts of intact PNA are excreted into the bladder. along with some protein fragments, and free radioiodide from the in vivo deiodination of the protein.

Recently several investigators have used FITC-, rhodamine-, and horseradish peroxidase- (HRP) labeled PNA as specific histochemic reagents for the investigation of the localization of galactosyl residues in glycoconjugates in the cell organelles and cell surfaces, elucidation of transport mechanisms of individual cell types in renal epithelia, and as a biochemic probe to demonstrate the morphologic and functional heterogenicity of the nephron (*9–13*). In frozen tissue sections, with direct application of PNA, considerable species variation in kidney PNA binding sites has been demonstrated (*12*), however, in the dog and rabbit the most common binding has been to the luminal brush border of distal tubules. Glomerular binding has been demonstrated when the sections were treated with neuraminidase, an enzyme which removes sialic acid from glycoproteins, however, not in untreated sections. The same phenomenon has recently been shown to occur in Haemolytic-Uraemic syndrome (HUS) due to the presence of neuraminidase from pneumococcal infections (*22*). HRP-PNA binding studies in perfused cortical collecting ducts of rabbit nephrons have revealed strong affinity of the lectin for intercalated tubular cells, but not for the adjacent principal cells (*13*). These results, however, are obtained from tissue sectioning studies where PNA was incubated with the cut sections.

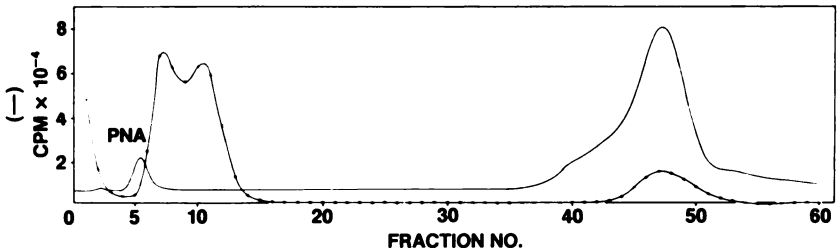

FIGURE 2
Gel column chromatography profile (Biogel P150, 2.5 × 50 cm) of dog urine 1 hr p.i. of 200 μg/35 MBq [^{131}I] PNA. (O—O) = Radioactivity (I-131); (—) = uv Absorbance at 280 nm

TABLE 3
Urine Analysis Following [^{131}I]PNA Administration in Dogs (Mean ± s.d., N = 4)

Collection period (hr)	% Inj. dose	% Protein-bound radioactivity (TCA)	% Immunoreactivity (A-GM$_1$ synsorb binding)
0–1	14.3 ± 2.1	92.4 ± 2.1	67.1 ± 4.2
1–3	15.8 ± 4.9	90.7 ± 4.0	60.2 ± 5.4
3–6	13.7 ± 3.2	75.4 ± 5.2	51.8 ± 6.2
6–9	11.8 ± 1.9	59.3 ± 4.1	35.4 ± 4.1
9–24	9.9 ± 2.0	23.1 ± 2.7	18.6 ± 2.9
24–48	8.1 ± 3.2	15.2 ± 3.1	11.2 ± 3.2
Cumulative 48-hr urine excretion	73.5 ± 9.8		

These techniques may expose many luminal structures that would not be in contact with capillary circulated PNA. Although morphologic differences in various species have been shown with PNA binding in tissue sections, we have not observed any major kinetic differences in renal clearance of i.v. injected [^{131}I]PNA in dogs or rabbits. Humans vary in that time-to-peak estimates are prolonged (*15*). Slight changes in the relative staining intensity of cortical and medullary tubules were seen between the animal species, however, the morphologic patterns were similar.

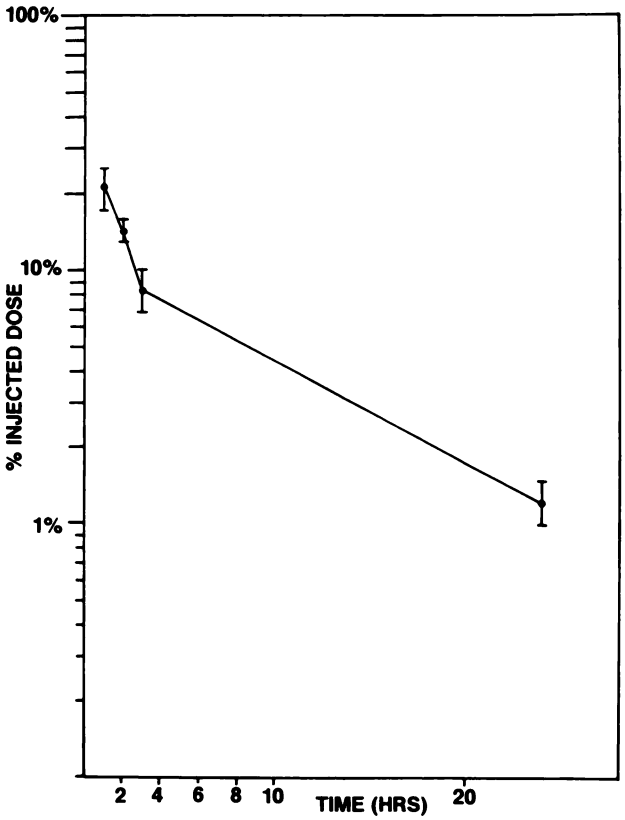

FIGURE 3
Gamma camera static image estimates of % injected dose remaining in kidneys vs. time in dogs after [^{131}I]PNA injection (mean ± s.d., N = 4)

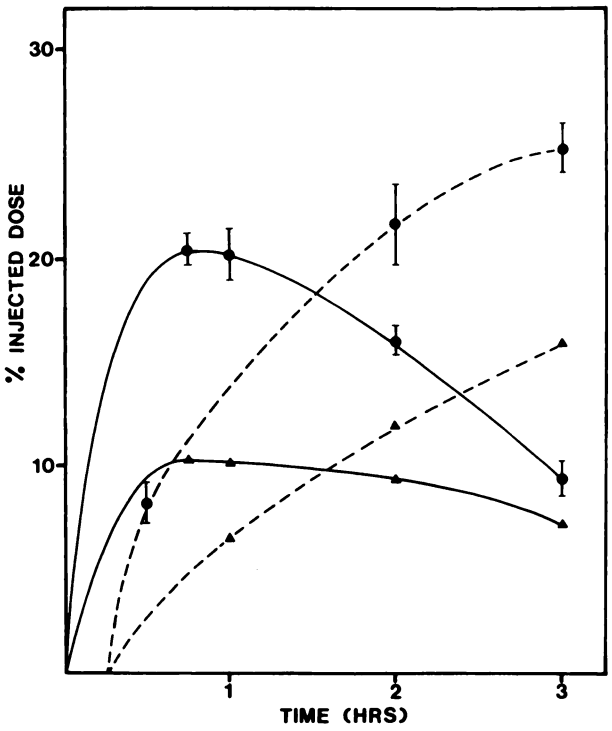

FIGURE 4
Dynamic kidney and bladder curves of control vs. D-galactose-infused dogs (2.5 g loading dose, 50 mg/min). (●) Normals; (▲) D-GAL-injection; (—) Kidneys; (---) Bladder

Our results suggest that when PNA is perfused into the kidney by plasma, there is strong affinity for the lectin by the basement membrane of renal tubules, predominantly in the cortex of the kidney. Moreover, this affinity appears to be competitively inhibited by the concomitant infusion of D-galactose, a known competitive inhibitor of the galactosyl binding sites of PNA. This would indicate that T-F antigen or T-F antigen-like receptors exist on the basement membrane of these tubules and that such receptors play an important role in the excretion of [^{131}I]PNA from plasma. Once association with the tubule occurs, PNA is secreted into the lumen of the nephron and subsequently into the bladder. No kidney retention of activity could be demonstrated in our study that would indicate reabsorption, although focal luminal staining of collecting ducts was seen. Tissue section studies have revealed the presence of PNA binding sites on the luminal surface of the nephron, particularly on intercalated cells (*13*). Our results confirm this finding, however, they would suggest that the sites do not act as renal fixation sites for PNA, as activity was noted to diminish with time.

The discovery of intact PNA in the urine contents is an important finding, indicating a unique secretory process of large molecular weight proteins by renal tubules. There is some degree of degradation during excretion, resulting in smaller molecular weight protein

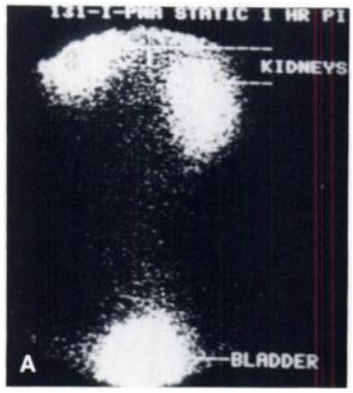

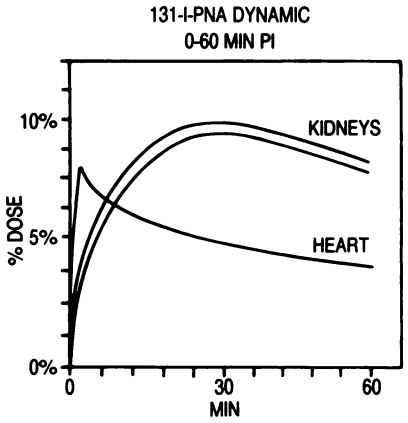

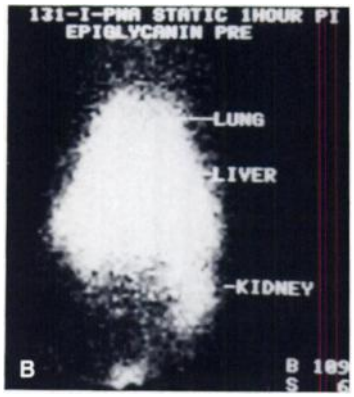

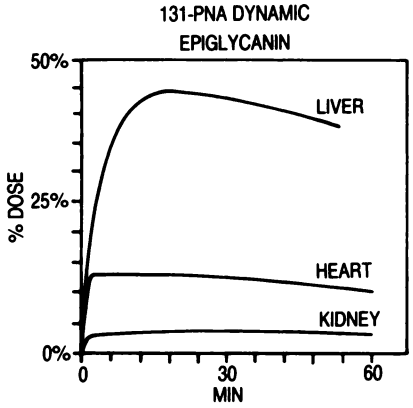

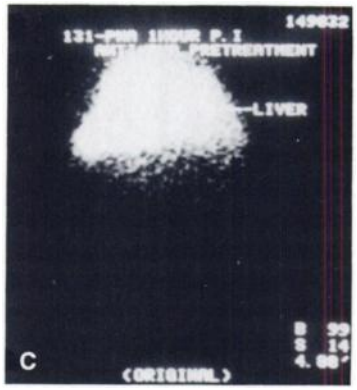

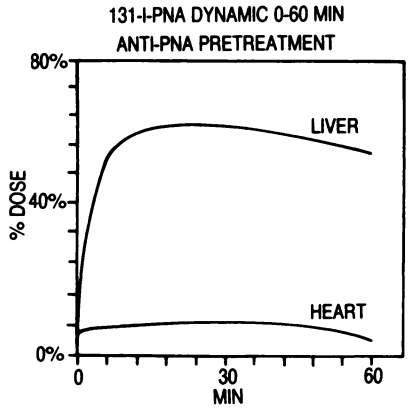

FIGURE 5
Static scintiphotos 1 hr p.i. and 0–60-min dynamic curves in rabbits. A = Untreated animals; B = Epiglycanin (120 μg i.v.) pretreatment; C = Anti-PNA (160 μg i.v.) pretreatment

fragments, however, the majority is functionally intact with respect to asialo-GM_1 synsorb binding at early times (<3 hr p.i.). This excretion appears to be inert to pharmacologic intervention by probenecid.

The biodistribution of [^{131}I]PNA is significantly altered when epiglycanin is administered 60 min prior to injection. Epiglycanin is a 500,000 mol wt glycoprotein containing ~520 O-glycosyl-linked carbohydrate chains (*23*). This glycoprotein is derived from the TA3/Ha ascites murine tumor line and is found in the serum and ascites fluid of mice bearing this tumor (*25*). There is strong evidence that the T-F hapten (β-D-Gal-(1 → 3)-α-GalNAc) is a major component of epiglycanin (*23*). Lectin binding sites on liver hepatocytes and Kupffer cells are thought to remove asialo glycoproteins such as epiglycanin from the plasma (*25–27*) and this mechanism appears to contribute to the removal of [^{131}I]PNA from plasma in pretreated animals, presumably by the formation of lectin-glycoprotein complexes. It is uncertain at present whether the interaction of [^{131}I]PNA with epiglycanin occurs in plasma and the complex is subsequently removed by the liver, or whether this interaction occurs on the membrane surface of the liver cells. Localization of the complex is also noted in the lungs where alveolar macrophages are also known to express receptors for glycoproteins and glycoconju-

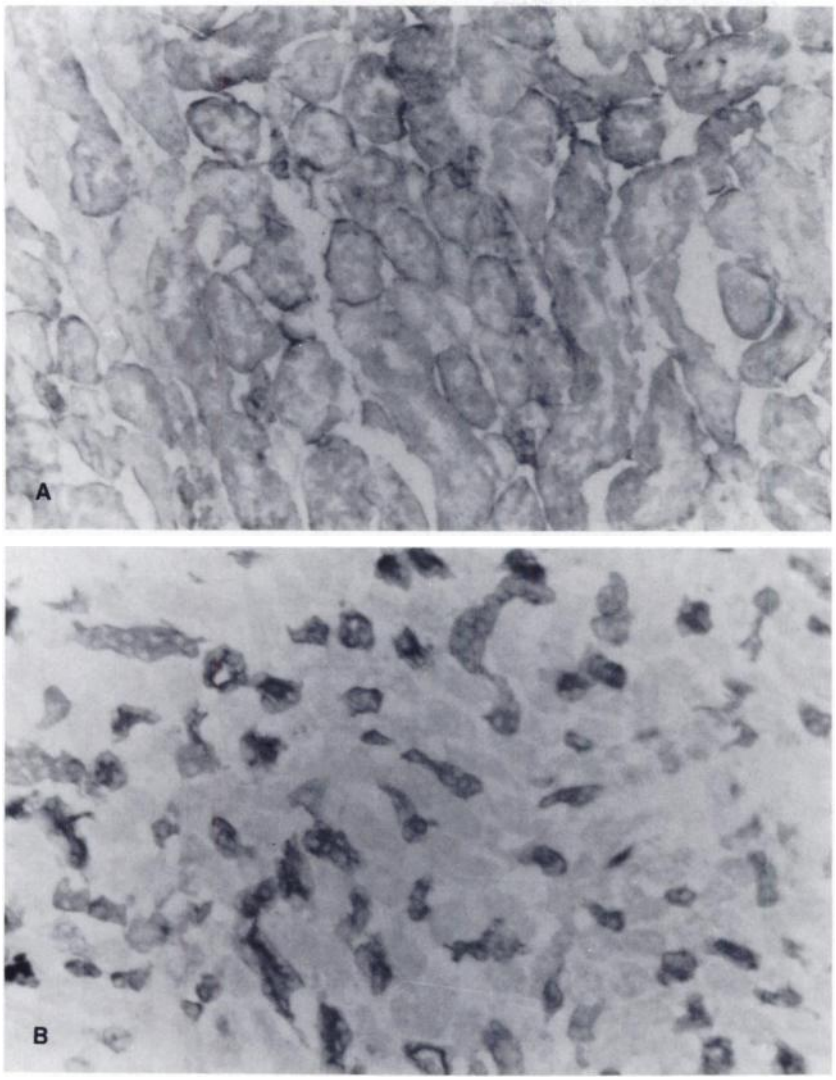

FIGURE 6
A: Frozen section of outer cortex mouse kidney stained by immunoperoxidase method (1 hr p.i. 10 μg PNA i.v.). Cytoplasm of proximal convolute tubular cells stain diffusely positive with prominent accentuation of the outer membrane of the tubular epithelial cell (DAB substrate, no counterstain). B: Frozen section of the outer medulla mouse kidney (1 hr p.i. 10 μg PNA i.v.). Strong cytoplasmic staining with slight membrane accentuation of outer membrane and focal luminal staining of proximal collecting ducts. Other medullary tubules were not stained (DAB substrate, no counterstain)

gates (*28*), although mechanical trapping of aggregates cannot be excluded. After the initial association with liver, there is a diminution in liver activity at later time frames. This indicates a temporary association of the complex with the liver, however, it is uncertain whether intact [^{131}I]PNA or free ^{131}I is released back into the circulation. Iodine-131 PNA is also removed rapidly by the liver when antibodies against PNA are present in the circulation. The dynamic pattern indicates a more stable association of the PNA-anti PNA complex with the liver than that seen with the PNA-epiglycanin complex.

Because of the rapid excretion of [^{131}I]PNA by the renal tubules after i.v. injection, this agent may show promise for the quantitation of renal tubular function. Existing agents such as [^{131}I]*o*-hippurate have some limitations in this respect due to their mixed excretion characteristics, however, the clinical usefulness of [^{131}I] PNA in renal disease has not yet been fully evaluated. Although accurate quantification of the plasma clearance of [^{131}I]PNA is complicated by the competing release of free iodide in vivo the quantitative analysis of the renal uptake, by standard radionuclide renographic techniques, may offer an accurate gauge of renal tubular function. This procedure would require analysis of renal activity within the first 60–90 min p.i., time points where the radiolabel is relatively stable. Alternatively, the development of methods for labeling PNA with indium-111, gallium-67 (by way of bifunctional chelates), or technetium-99m, may reduce or eliminate the in vivo stability problems associated with iodinated PNA. These alternatives would also significantly reduce the radiation dose to the patient, allowing the administration of higher doses and result in better counting statistics for dynamic studies.

Because PNA is a protein of nonhuman origin, some reservations have been expressed concerning the antigenic properties of this agent. We have shown that biodistribution is drastically altered by the presence of anti-PNA IgG antibodies in plasma resulting in predominant liver localization and diminished kidney excretion. However, with chronic repeated i.v. adminis-

tration of PNA (400 mg/kg/wk) into mice over a prolonged period (1 mo), we have not been able to demonstrate significant antibody production that changes the biodistribution as demonstrated above (*19*), nor have we been able to demonstrate any toxicity with acute administration of 1,000-fold excesses of PNA in mice (*17*). The utility of radiolabeled peanut lectin for renal tubular function studies remains to be fully determined.

FOOTNOTES

* Chembiomed, Edmonton, Alberta, Canada.
† Pierce Chemical Co., Rockford, IL.
‡ A.E.C.L. Ottawa, Ontario, Canada.
§ Bio-Rad, Richmond, CA.
¶ Searle PhoGamma IV, high-energy parallel hole collimator.
** Sigma Chemical Co., St. Louis, MO.
†† Lab-Tek Products, Naperville, IL.
‡‡ Vector Laboratories Inc., Burlingome, CA.

ACKNOWLEDGMENTS

The authors thank the Alberta Cancer Board and the Alberta Heritage Foundation for Medical Research for their generous financial support. They also thank Dr. D. Baker (Chembiomed) for the supply of affinity-purified PNA and asialo-GM_1 synsorb.

REFERENCES

1. Springer GF, Desai PR, Banatwala I: Blood group M N antigens and precursors in normal and malignant human breast glandular tissues. *J Natl Cancer Inst* 54:335–339, 1975
2. Springer GF, Desai PR, Murthy MS, et al: Human carcinoma-associated precursor antigens of blood group M N system and the hosts immune response to them. *Prog Allergy* 26:42–46, 1979
3. Vos GH, Brain P: Heterophile antibodies, immunoglobulin levels and the evaluation of anti-T activity in cancer patients and controls. *S Afr Med J* 60:133–136, 1981
4. Noujaim AA, Shysh A, Zabel P, et al: The Thomsen-Friedenreich Antigen: an important marker for the radiodetection of cancer using macromolecular probes. In *Radioimmunoimaging and Radioimmunotherapy*, Burcheil SW, Rhodes BA, eds. Elsevier, Amsterdam, 1983
5. Kim Z, Uhlenbruck G: Untersuchen uber T-antigen un T-agglutinin. *Z Immunitaestsforesch Immunobiol* 130:88–89, 1966
6. Nakahara K, Ohashi T, Oda T, et al: Asialo-GM_1 as a cell surface marker detected in acute lymphoblastic leukemia. *N Engl J Med* 302:674–677, 1980
7. Springer DF, Murthy MS, Desai, et al: Patients immune response to breast and lung carcinoma associated Thomsen-Freidenreich (T) specificity. *Klin Wochenschr* 60:121–131, 1982
8. Ratcliffe RM, Baker DA, Lemieux RU: Synthesis of the T (asialo-GM_1) antigenic determinant in a form useful for the preparation of an effective artificial antigen and the corresponding immunoadsorbent. *Carbohydr Res* 93:35–41, 1981
9. Stoward PJ, Spicer SS, Millar RL: Histochemical reactivity of peanut lectin—Horseradish peroxidase conjugate. *J Histochem Cytochem* 28:979–990, 1980
10. LeHir M, Dubach UC: The cellular specificity of lectin binding in the kidney. I. Light microscopical study in the rat. *Histochemistry* 74:521–530, 1982
11. LeHir M, Dubach UC: The cellular specificity of lectin binding in the kidney. II. Light microscopical study in the rabbit. *Histochemistry* 74:531–540, 1982
12. Hölthofer H: Lectin binding sites in the kidney. *J Histochem Cytochem* 31:531–537, 1983
13. LeHir M, Kaisling B, Koeppen BM, et al: Binding of peanut lectin to specific epithelial cell types in kidney. *Am J Physiol* 242:117–120, 1982
14. Zabel PL, Noujaim AA, Shysh A, et al: Radioiodinated peanut lectin, a potential radiopharmaceutical for immunodetection of carcinoma expressing the T-antigen. *Eur J Nucl Med* 8:250–254, 1983
15. Holt S, Wilkinson AA, Suresh MR, et al: Radiolabelled peanut lectin for the scintigraphic detection of cancer. *Cancer Lett* 25:55–60, 1984
16. Abdi EA, Kamitomo VJ, Catz Z, et al: Radioiodinated peanut lectin: Clinical use, a tumour imaging agent and potential use in assessing renal tubular function. *Eur J Nucl Med*: in press
17. Shysh A, Eu SM, Noujaim AA, et al: In vivo localization of radioiodinated peanut lectin in a murine TA3/Ha mammary carcinoma model. *Eur J Nucl Med* 10:68–74, 1985
18. Shysh A, Eu SM, Noujaim AA, et al: Radioimmunodetection of murine mammary adenocarcinoma (TA3/Ha) lung and liver metastases with radioiodinated PNA. *Int J Cancer* 35:113–119, 1985
19. Shysh A, Boniface GR, Eu SM, et al: Kidney uptake of ^{125}I-peanut lectin in mice. *Proceedings of the Fourth International Symposium on Radiopharmacology*, Banff, Sept. 1985
20. Gibaldi M, Perrier D: *Pharmacokinetics*, 2nd Edition, New York, Marcel Dekker, Inc., 1982
21. Zabel PM: ^{125}I-Antibodies and PNA for tumour detection. MSc Thesis, University of Alberta, 1982
22. Klein PJ, Bulla M, Newman RA, et al: The significance of pneumococcal neuraminidase for the development of Haemolytic Uraemic syndrome. In *Dialysis and Kidney Transplantation in Children*, Bulla M, ed. Bibliomed, Melsungen, 1979, pp 183
23. Van den Eijnden DH, Evans NA, Codington JF, et al: Chemical structure of epiglycanin, the major glycoprotein of the TA3-HA ascites cell. *J Biol Chem* 254:12153–12159, 1979
24. Millar DK, Cooper AG: Kinetics of release of glucosamine-labelled glycoproteins from the TA3-HA murine adenocarcinoma cells. *J Biol Chem* 253:8798–8803, 1978
25. Kolb-Bachofen V, Schelepper-Schafer J, Vogell, et al: Electron microscopic evidence for an asialoglycoprotein receptor on Kupffer cells: Localization of lectin mediated endocytosis. *Cell* 29:859–866, 1982
26. Ashwell G, Harford J: Carbohydrate-specific receptors of the liver. *Ann Rev Biochem* 51:531–554, 1982
27. Steer CJ, Ashwell G: Studies on a mammalian hepatic binding protein specific for asialo glycoproteins. *J Biol Chem* 255:3008–3013, 1980
28. Stahl PD, Rodman JS, Millar MJ, et al: Evidence for receptor-mediated binding of glycoproteins, glycoconjugates and lysosomal glycosidases by alveolar macrophages. *Proc Natl Acad Sci* 75:1399–1403, 1978